

A Phase Shift Deep Neural Network for High Frequency Wave Equations in Inhomogeneous Media

Wei Cai^a, Xiaoguang Li^{b,a}, Lizuo Liu^a

^a*Department of Mathematics, Southern Methodist University, Dallas, TX 75275, USA.*

^b*LCSM, Ministry of Education, School of Mathematics and Statistics, Hunan Normal University, Changsha, Hunan 410081, P. R. China*

Abstract

In this paper, we propose a phase shift deep neural network (PhaseDNN) which provides a wideband convergence in approximating high frequency solutions of wave equations. The PhaseDNN accounts for the fact that many DNN achieves convergence in the low frequency range first, a series of moderately-sized of DNNs are constructed and trained for selected high frequency ranges. With the help of phase shifts in the frequency domain, each DNN will be trained to approximate the target solution's higher frequency content over a specific range. Due to the phase shift, each DNN achieves the speed of convergence as in the low frequency range. As a result, the proposed PhaseDNN is able to convert high frequency learning to low frequency learning, thus allowing a uniform learning to wideband high frequency functions. The PhaseDNN will then be applied to find the solution of high frequency wave equations in inhomogeneous media. Numerical results have demonstrated the capability of PhaseDNN in learning high frequency functions and oscillatory solutions of Helmholtz equations.

Keywords: Neural network, phase shift, wideband data, high frequency waves, Helmholtz equations

1. Introduction

High frequency wave scattering in inhomogeneous media, arising from various application such as seismic waves, geophysical problems, poses great computational challenges due to the highly oscillatory natures of the solutions as well as the variance of random media properties. To model the high frequency waves in a deterministic media, high order methods such as spectral

methods for the differential equations or wideband fsat multipole methods for the integral equations are used. Sparse grid methods have been used to reduce the cost of simulation over the high dimensional random spaces, however, these methods still suffer the curse of dimensionality.

Deep neural network (DNNs) have shown great potential in approximating high dimensional functions compared with traditional approximations based on Lagrangian interpolation or spectral methods. Recently, it has been shown in [3, 4] that some common NNs, including fully connected and convolution neural network (CNN) with tanh and ReLU activation functions, demonstrated a frequency dependent convergence behavior, namely, the DNNs during the training are able to approximate the low frequency components of the targeted functions first before than the higher frequency components, named as the F-Principle of DNNs [3]. The stalling of DNN convergence in the later stage of training could be mostly coming from learning the high frequency components of the data. This F-principle behavior of DNN is just the opposite to that of the traditional multigrid method (MGM) [5] in approximating the solutions of PDEs where the convergence occurs first in the higher frequency end of the spectrum, due to the smoothing operator employed in the MGM. The MGM takes advantage of this fast high frequency error reduction in the smoothing iteration cycles and restrict the original solution of a fine grid to a coarse grid, then continuing the smoothing iteration on the coarse grid to reduce the higher end frequency spectrum in the context of the coarse grid. This downward restriction can be continued until errors over all frequency are reduced by a small number of iteration on each level of the coarse grids.

Our object is to develop DNNs based numerical methods to handle high frequency functions and solutions of high frequency wave equation in inhomogeneous media, whose solution will be oscillatory and high dimensional functions due to the random coefficients. For this purpose, we will have to develop new classes of DNNs with capability of representing highly oscillatory solutions in the physical spatial variables, at the same time, addressing the challenging of representing high random space dimensions.

In this paper, we will consider the following Helmholtz equations PDE in an inhomogeneous media

$$\nabla^2 u + (\lambda^2 + \omega(x)) u = f(x), \quad x \in \Omega \subset R^d, \quad (1)$$

with appropriate boundary condition on $\partial\Omega$ for a bounded domain plus a

radiation condition at ∞ for an exterior scattering problem.

Our goal is to hopefully find a DNN parameterized by θ approximation to

$$T(x, \theta) \sim u(x), x \in R^d. \quad (2)$$

To improve the capability of usual DNNs for learning highly oscillatory functions in the physical variable \mathbf{x} , we propose phase shift DNNs with wide-band learning capabilities in error reductions in the approximation for all frequencies of the targeted function by making use of the faster convergence in the low frequencies of the DNN during its training. We approximate the target function with a series of functions with disjoint frequency spectrum through a partition of the unit (POU) in the k -space. To learn each of these function of specific frequency range, we employ a phase shift in the k -space to translate its frequency to the range $|k| < K_0$, then the phase shifted function now only has low frequency content and can be learned by common DNNs with a small number of epoches of training. This series of DNNs with phase shifts will be named phase shift deep neural network (PhaseDNN).

To achieve this wideband approximation of a function, we can implement the PhaseDNN in a parallel manner where each range of frequency of the training data, after a proper phase shift, is learned independently. This approach can take advantage of parallel implementation, however, frequency extraction of the original training data have to be done using convolution with a frequency selection kernel numerically, which could become expensive or not accurate for scattered training data. Alternatively, we can also implement the PhaseDNN in a non-parallel manner where data from all range of frequencies are learned together with phase shifts included in the PhaseDNN, which will be called coupled PhaseDNN. Although, the coupled PhaseDNN lacks the parallelism of the parallel PhaseDNN, it avoids the costly convolution used in the parallel PhaseDNN to extract the frequency component from the original training data. This feature will be shown to be important when higher dimensional data are involved in the training. Due to this property, the coupled PhaseDNN will be used to solve the high frequency wave problems where we will seek solutions in a space of PhaseDNN by minimizing the residuals of the differential equation.

The rest of the paper will be organized as follows. In section 2, we will review the fast low frequency convergence property of neural network with tanh activation function. Section 3 will present the parallel version phase shift deep neural network - PhaseDNN. Based on the properties of the

PhaseDNN, a coupled PhaseDNN is introduced in Section 4 to reduce the cost of learning in training the DNN for approximations. Then, the coupled PhaseDNN is used to solve the differential equation for wave propagation. Section 5 contains various numerical results of the PhaseDNN for approximations and solutions of wave problems by differential equations. Finally, a conclusion and discussions will be given in Section 6.

2. Deep Neural Network and frequency dependent training of DNN

A deep neuron network (DNN) is a sequential alternative composition of linear functions and nonlinear activation functions. Given $m, n \geq 1$, let $\Theta(\mathbf{x}) : \mathbb{R}^n \rightarrow \mathbb{R}^m$ is a linear function with the form $\Theta(\mathbf{x}) = \mathbf{W}\mathbf{x} + \mathbf{b}$, where $\mathbf{W} = (w_{ij}) \in \mathbb{R}^{n \times m}$, $\mathbf{b} \in \mathbb{R}^m$. The nonlinear activation function $\sigma(u) : \mathbb{R} \rightarrow \mathbb{R}$. By applying this function componentwisely, we can extend activation function to $\sigma(u) : \mathbb{R}^n \rightarrow \mathbb{R}^n$ naturally. A DNN with $L + 1$ layers can be expressed as a compact form

$$\begin{aligned} T(\mathbf{x}) &= T^L(\mathbf{x}), \\ T^l(\mathbf{x}) &= [\Theta^l \circ \sigma](T^{l-1}(\mathbf{x})), \quad l = 1, 2, \dots, L, \end{aligned} \quad (3)$$

with $T^0(\mathbf{x}) = \Theta^0(\mathbf{x})$. Equivalently, we can also express it explicitly:

$$T(\mathbf{x}) = \Theta^L \circ \sigma \circ \Theta^{L-1} \circ \sigma \dots \circ \Theta^1 \circ \sigma \circ \Theta^0(\mathbf{x}). \quad (4)$$

Here, $\Theta^l(\mathbf{x}) = \mathbf{W}^l \mathbf{x} + \mathbf{b}^l : \mathbb{R}^{n^l} \rightarrow \mathbb{R}^{n^{l+1}}$ are linear functions. This DNN is also said to have L hidden layers. The l -th layer has n^l neurons.

In the following text, we only consider DNN with one dimensional input layer and one dimensional output layer. Namely, $\Theta^0(x) : \mathbb{R} \rightarrow \mathbb{R}^{n^1}$, $\Theta^L(\mathbf{x}) : \mathbb{R}^{n^{L-1}} \rightarrow \mathbb{R}$. That is, $T(\mathbf{x}) : \mathbb{R} \rightarrow \mathbb{R}$. The activation function is chosen to be $\sigma(u) = \tanh(u)$.

In this paper, we consider the problem of approximating a function by DNN through training. Given a function $f(x) \in \mathbb{L}^1(\mathbb{R}) \cap \mathbb{L}^2(\mathbb{R})$ (This choice is only to ensure the existence of Fourier transform and loss function for analysis reason.), we are going to minimize

$$L(\mathbf{W}^0, \mathbf{b}^1, \mathbf{W}^1, \mathbf{b}^1, \dots, \mathbf{W}^L, \mathbf{b}^L) = \|f(\mathbf{x}) - T(\mathbf{x})\|_2^2 = \int_{-\infty}^{+\infty} |f(\mathbf{x}) - T(\mathbf{x})|^2 x. \quad (5)$$

We consider this problem in frequency space. We define Fourier transform and its inverse of a function $f(\mathbf{x})$ by

$$\mathcal{F}[f](k) = \frac{1}{\sqrt{2\pi}} \int_{-\infty}^{+\infty} f(x) e^{-ikx} dx, \quad \mathcal{F}^{-1}[\hat{f}](x) = \frac{1}{\sqrt{2\pi}} \int_{-\infty}^{+\infty} \hat{f}(k) e^{ikx} dk. \quad (6)$$

Let $D(k) = \mathcal{F}[T - f](k) = A(k)e^{i\varphi(k)}$, $L(k) = |D(k)|^2$. By Parseval's equality,

$$L(\mathbf{W}^0, \mathbf{b}^1, \mathbf{W}^1, \mathbf{b}^1, \dots, \mathbf{W}^L, \mathbf{b}^L) = \int_{-\infty}^{+\infty} L(k) k. \quad (7)$$

Let θ denotes all the parameters in DNN. Namely,

$$\theta = (\mathbf{W}_1^0, \mathbf{W}_2^0 \dots, \mathbf{W}_{n^1}^0, \mathbf{b}^0, \mathbf{W}_{11}^1, \dots, \mathbf{W}_{n^1 n^2}^1, \mathbf{b}_1^1 \dots \mathbf{b}_{n^2}^1 \dots) \in \mathbb{R}^p.$$

Here, $p = n^1 + 1 + (n^1 + 1) \times n^2 + (n^2 + 1) \times n^3 + \dots (n^L + 1)$ is the number of the parameters. The F-principle states the relative changing rate of $\frac{\partial L(k)}{\partial \theta_j}$ for different frequency k . We cite the following result from [4]

Theorem 1. *Given a function $f(\mathbf{x}) \in \mathbb{L}^1(\mathbb{R}) \cap \mathbb{L}^2(\mathbb{R})$ and a DNN function $T(\mathbf{x})$ defined by (3), we scale $T(\mathbf{x})$ by $\Theta^0(\mathbf{x}) = \varepsilon \mathbf{W}^0 \mathbf{x} + \mathbf{b}$, where $\varepsilon > 0$ is a small parameter. Suppose $\mathbf{W}_{rs}^l \neq 0$ for all $0 \leq l \leq L - 1$, $1 \leq r \leq n^l$ and $1 \leq s \leq n^{l+1}$. For any frequency k_1 and k_2 such that $|\mathcal{F}[f](k_1)| > 0$, $|\mathcal{F}[f](k_2)| > 0$ and $|k_2| > |k_1| > 0$, there exists a $\delta > 0$ such that when $\varepsilon < \delta$,*

$$\frac{\mu \left(\left\{ \theta \mid \left| \frac{\partial L(k_1)}{\partial \theta_j} \right| > \left| \frac{\partial L(k_2)}{\partial \theta_j} \right| \right\} \cap B_\delta \right)}{\mu(B_\delta)} > 1 - C \exp(-c/\delta)$$

holds for all j , where $B_\delta = \{\mathbf{x} \in \mathbb{R}^p \mid |\mathbf{x}| < \delta\}$, $\mu(\cdot)$ is the Lebesgue measure and $c > 0$, $C > 0$ are two constants.

3. A parallel phase shift DNN (PhaseDNN)

The F-principle and estimation of $L(k)$ in Theorem 1 suggest that when we apply a gradient-based training method to loss function, the low frequency part of loss function converges faster than the high frequency part. So when we train a DNN $T_\star(x)$ to approximate $f(x)$, there exists positive frequency number K_0 and an integer n_0 such that after n_0 steps of training, the Fourier transform of training function $\mathcal{F}[T_\star](\mathbf{k}; \theta^{(n_0)})$ should be a good approximation of $\mathcal{F}[f](\mathbf{k})$ for $|k| < K_0$, where $\theta^{(n_0)}$ are parameters obtained after n_0 steps of training.

- Frequency selection kernel $\varphi_j^\vee(x)$

Following [6], in order to speed up the learning of the higher frequency content of the target function $f(x)$, we will employ a phase shift technique to translate higher frequency spectrum $\widehat{f}(k)$ to the frequency range of $[-K_0, K_0]$. Such a shift in frequency is a simple phase factor multiplication on the training data in the physical space, which can be easily implemented.

For a given Δk , let us assume that

$$\text{supp } \widehat{f}(k) \subset [-m\Delta k, m\Delta k].$$

Before we can carry out this scheme, we construct a mesh for the interval $[-m\Delta k, m\Delta k]$ by

$$\omega_j = j\Delta k, j = -m, \dots, m, \quad (8)$$

Then, we introduce a POU for the domain $[-M, M]$ associated with the mesh as

$$1 = \sum_{j=0}^m \varphi_j(k), \quad k \in [-M, M]. \quad (9)$$

The simplest choice of $\varphi_j(k)$ is

$$\varphi_j(k) = \varphi\left(\frac{k - \omega_j}{\Delta k}\right), \quad (10)$$

where $\varphi(k)$ is just the characteristic function of $[-1, 1]$, i.e.,

$$\varphi(k) = \chi_{[0,1]}(k).$$

The inverse Fourier transform of $\varphi(k)$, indicated by \vee , is

$$\varphi^\vee(x) = \frac{1}{\sqrt{2\pi}} e^{i\frac{x}{2}} \frac{\sin x}{x}. \quad (11)$$

For a smoother function $\varphi(k)$ whose inverse Fourier transform, which will act as a frequency selection kernel in x -space, has a faster decay condition, we could use B-Splines $B_m(k)$, defined by the following recursive convolutions. Namely,

$$B_1(k) = \chi_{[0,1]}(k),$$

$$B_m(k) = B_{m-1}(k) * \chi_{[0,1]}(k), m = 2, \dots. \quad (12)$$

It can be easily shown that

$$\text{supp } B_m(k) = [0, m],$$

and the inverse Fourier transform of $B_m(k)$ is

$$\begin{aligned} B_m^\vee(x) &= (B_1^\vee(x))^m = \left(\frac{1}{\sqrt{2\pi}} e^{i\frac{x}{2}} \frac{\sin \frac{x}{2}}{\frac{x}{2}} \right)^m \\ &= \frac{e^{i\frac{mx}{2}}}{(2\pi)^{m/2}} \left(\frac{\sin \frac{x}{2}}{\frac{x}{2}} \right)^m. \end{aligned}$$

In most cases, we will just use the cubic B-Spline. We choose

$$\varphi(k) = B_4(k+2), \quad (13)$$

and $\varphi_j(k) = \varphi(k/\Delta k - j)$. Therefore,

$$\varphi^\vee(x) = \frac{1}{(2\pi)} \left(\frac{\sin \frac{x}{2}}{\frac{x}{2}} \right)^4 = O\left(\frac{1}{|x|^4}\right) \text{ as } x \rightarrow \infty,$$

which defines the *frequency selection kernel*

$$\varphi_j^\vee(x) = e^{-ij\Delta kx} \varphi^\vee(\Delta kx) = e^{-ijK_0x} \varphi^\vee(K_0x), \Delta k = K_0,$$

and

$$\text{supp } \mathcal{F}[\varphi_j^\vee(x)] \subset [\omega_{j-2}, \omega_{j+2}].$$

From the basic property of B-spline functions, we know that

$$\sum_{j \in \mathbb{Z}} \varphi_j(k) = \sum_{j \in \mathbb{Z}} B_4\left(\frac{k}{\Delta k} + 2 - j\right) \equiv 1, \quad \forall k \in \mathbb{R}.$$

Thus,

$$\sum_{j=-m-1}^{m+2} \varphi_j(k) = 1, \quad \forall k \in [-m\Delta k, m\Delta k]. \quad (14)$$

In Eqn. (14), we define $\varphi_{-m-1} = B_4(k/\Delta k + m + 3)$, $\varphi_m = B_4(k/\Delta k - m + 2)$ and $\varphi_{m+1} = B_4(k/\Delta k - m + 1)$.

Now, with the POU in (9), we can decompose the target function $f(x)$ in the Fourier space as follows,

$$\widehat{f}(k) = \sum_{j=-m}^m \varphi_j(k) \widehat{f}(k) \triangleq \sum_{j=-m}^m \widehat{f}_j(k). \quad (15)$$

Equation (15) will give a corresponding decomposition in x -space

$$f(x) = \sum_{j=-m}^m f_j(x), \quad (16)$$

where

$$f_j(x) = \mathcal{F}^{-1}[\widehat{f}_j](x).$$

The decomposition (16) involves $m + 1$ function $f_j(x)$ whose frequency spectrum is limited to $[\omega_{j-1}, \omega_{j+1}]$, therefore, a simple phase shift could translate its spectrum to $[-K_0, K_0]$, then it could be learned quickly by a DNN with n_0 training epoches.

- A parallel phase shift DNN (PhaseDNN) algorithm

Our goal is to learn function $f(x)$ based on its training data

$$\{x_i, f_i = f(x_i)\}_{i=1}^N. \quad (17)$$

In order to learn $f(x)$ for its frequency information for all frequencies uniformly, we will apply the decomposition (16) to $f(x)$

$$f(x) = \sum_{j=-m}^m f_j(x), \quad (18)$$

where

$$f_j(x) = \mathcal{F}^{-1}[\widehat{f}_j(k)] = \mathcal{F}^{-1}[\varphi_j(k) \widehat{f}(k)](x). \quad (19)$$

The training data for $\{f_j(x_i)\}_{i=1}^N$ will be computed by (19), which can be implemented in the data x -space through the following convolution

$$\begin{aligned}
f_j(x_i) &= \varphi_j^\vee * f(x_i) = \int_{-\infty}^{\infty} \varphi_j^\vee(x_i - s) f(s) ds \\
&\approx \frac{2\delta}{N_s} \sum_{x_s \in (x_i - \delta, x_i + \delta)} \varphi_j^\vee(x_i - x_s) f(x_s),
\end{aligned} \tag{20}$$

where δ is chosen such that the kernel function |

Now as the support of $\widehat{f}_j(k)$ is $[\omega_{j-1}, \omega_{j+1}]$, then $\widehat{f}_j(k - \omega_j)$ will have its frequency spectrum in $[-\Delta k, \Delta k] = [-K_0, K_0]$, therefore its inverse Fourier transform $\mathcal{F}^{-1}[\widehat{f}_j(k - \omega_j)]$, denoted as

$$f_j^{\text{shift}}(x) = \mathcal{F}^{-1}[\widehat{f}_j(k - \omega_j)](x), \tag{21}$$

can be learned quickly by a DNN

$$T_j(x, \theta^{(n_0)}) \approx f_j^{\text{shift}}(x), 0 \leq j \leq m, \tag{22}$$

in n_0 -epoches of training. Moreover, we know that

$$f_j^{\text{shift}}(x_i) = e^{i\omega_j x_i} f_j(x_i), 1 \leq i \leq N, \tag{23}$$

which provides the training data for $f_j^{\text{shift}}(x)$. Equation (23) shows that once $f_j^{\text{shift}}(x)$ is learned, $f_j(x)$ is also learned by removing the phase factor.

$$f_j(x) \approx e^{-i\omega_j x} T_j(x, \theta^{(n_0)}). \tag{24}$$

Now all $r_j(x)$ $0 \leq j \leq m$ have been learned, we will have an approximation to $f(x)$ over all frequency range $[-M, M]$ as follows

$$f(x) \approx \sum_{j=-m}^m e^{-i\omega_j x} T_j(x, \theta^{(n_0)}). \tag{25}$$

Remark 1. *It should be noted that during the construction of PhaseDNN, only the original set of training data will be needed, but it will be modified to account for the frequency shifts, implemented simply by multiplying the training data by a phase factor $e^{\pm\omega_j x}$ on the residuals from the previous neural network approximations. We also allude the way PhaseDNN achieve approximation over increasing range of frequency with each additional network to*

that of wavelet approximations, which generate better and better resolution of approximation by adding wavelet subspaces produced by dialation of mother wavelet to account for higher frequency [7][8]. In the case of PhaseDNN though phase shifts are used to cover higher frequencies. The subtraction between the target function provided by the training data and the lower frequency network approximation is similar to the strategy employed in construction of multi-resolution interpolation for PDE solutions[8].

Remark 2. (Parallelism of PhaseDNN) It is clear the learning for each part of residual function $f_j(x)$ can be done in parallel, the PhaseDNN is a version of domain decomposition method in k -space.

Remark 3. (Frequency Adaptivity of PhaseDNN) The frequency-selected function $f_j(x_i)$ requires the evaluation of the convolution (20), which implicitly assumes sufficient data information is available in the neighborhood of x_i . In case such an assumption is not valid, we basically do not have enough data to extract the frequency information for the target function. In all practical sense of learning, we should assume the target function do not have the information of this specific frequency, and there is no need to learn this function $f_j(x)$ near x_i and we could simply set $f_j(x) = 0$ for $x \in (x_i - \delta, x_i + \delta)$, which is what could happen for a constant (or low) frequency function $f(x)$. As this process is done locally in space and frequency, the PhaseDNN will be able to achieve frequency adaptivity commonly associated with wavelet approximation of signals and images.

- **Adaptivity in frequency and local radial Basis fitting** A pre-analysis of the training data could be done to investigate the frequency content of the data, so only those frequencies will be considered when phase shifts are used for error reduction. Firstly, we group the training data x_i into N_c clusters (disjoint or overlapping). Secondly, in a sphere centered at the center of a cluster, a local radial basis function fitting of training data $\{x_i, y_i\}$ falling in the sphere will be carried out [9]. Finally, we apply an 1-D discrete Fourier transform over the fitting function along each coordinate direction within the cluster to get the frequency content for the data in the cluster. Once this analysis is done for each cluster, we will have a collection of frequencies and those with significant magnitude will be used as candidates for the phase shifts in the PhaseDNN.

Remark 4. (Selection of K_0 and n_0 and pre-processing training data) In principle, any nonzero frequency threshold K_0 can be used in the imple-

mentation of PhaseDNN, which will dictate the size of n_0 to achieve sufficient convergence of the underlying DNN over the frequency range $[-K_0, K_0]$. Therefore, a careful analysis and numerical experiment of the specific low frequency convergence of the DNN will be needed.

As n_0 is selected to train the initial network in PhaseDNN to learn low frequent content of the data, a low-pass filtering on the training data could be used to select appropriate size of n_0 needed for achieve convergence within K_0 frequency.

4. A coupled PhaseDNN

4.1. Approximations

In the last section, we use the frequency selection kernel $\varphi_j^\vee(x)$ to decompose the training data into different frequency components, each of them after being phase-shifted will be represented by a small DNN. This method can be implemented in parallel, however, has to use convolution to construct the training data for each small DNN. The convolution is equivalent to a matrix multiplication and the matrix requires a storage of $O(N \times N)$, N is the number of samples. As a result, this convolution process strongly restricts the performance of phase DNN for higher dimensions.

To avoid this problem, based on the construction of the parallel PhaseDNN (25), we would like to consider a coupled weighted phase-shifted DNNs as an ansate for a new DNN, termed as coupled PhaseDNN,

$$T(x) = \sum_{m=1}^M e^{i\omega_m x} T_m(x) \quad (26)$$

to approximate $f(x), x \in \mathbb{R}^d$, where $T_m(x)$ are relatively small DNNs, ω_m are frequencies we are particularly interested in. Namely, we are going to minimize

$$\|f(x) - T(x)\|_2^2 \approx \sum_{n=1}^N |f(x_n) - T(x_n)|^2 = \sum_{n=1}^N \left| f(x_n) - \sum_{m=1}^M e^{i\omega_m x_n} T_m(x_n) \right|^2. \quad (27)$$

This method is similar to expansion with Fourier modes of selected frequency with variable coefficients by DNNs. As $f(x)$ is a real function, it is

equivalent to use real "Fourier" series rather than complex "Fourier" series. Namely, we will consider the following sine and cosine expansions

$$T(x) = \sum_{m=1}^M A_m \cos(\omega_n x) + B_m \sin(\omega_n x) \quad (28)$$

to approximate $f(x)$, where A_m, B_m are DNNs while $\omega = 0$ will always be included.

4.2. Solving differential equations

We will apply the coupled PhaseDNN to solve differential equation for the interior wave problems. Eqn.(28) is a good ansatz for solving differential equation (DE).

The test problem is

$$\begin{cases} \mathcal{L}[u] \triangleq u'' + (\lambda^2 + c\omega(x))u &= f(x) \\ u(0) = 0, & u(1) = 0 \end{cases} \quad (29)$$

where the right hand side source function, representing external source, is taken to be

$$f(x) = (\lambda^2 - \mu^2) \sin(\mu x). \quad (30)$$

When $\omega(x) = 0$ and $\lambda \neq k\pi$, $\mu \neq \lambda$, the unique solution of the equation is

$$u(x) = -\frac{\sin \mu}{\sin \lambda} \sin(\lambda x) + \sin(\mu x). \quad (31)$$

Loss function $l(\theta)$. In finding the coupled PhaseDNN solution $T(x, \theta)$ to the DE, we use the residual of the DE to define the loss function as follows

$$l(\theta) = \sum_{i=1}^M |\mathcal{L}[T(\cdot, \theta)](x_i) - f(x_i)|^2. \quad (32)$$

5. Numerical results

5.1. Numerical result of parallel PhaseDNN for approximations

In this section, we will present some preliminary numerical results to demonstrate the capability of PhaseDNN to learn high frequency content of

target functions. In practice, we could sweep over all frequency ranges. For the test function we have some rough idea of the the range of frequencies in the data, only a few frequency intervals are selected for the phase shift.

We choose a target function $f(x)$ defined in $[-\pi, \pi]$ by

$$f(x) = \begin{cases} 10(\sin x + \sin 3x), & \text{if } x \in [-\pi, 0] \\ 10(\sin 23x + \sin 137x + \sin 203x), & \text{if } x \in [0, \pi]. \end{cases} \quad (33)$$

Because the frequencies of this function is well separated, we need not to sweep all the frequencies in $[-\infty, +\infty]$. Instead, we choose $\Delta k = 5$, and use the following functions

$$\begin{aligned} \varphi_1(k) &= \chi_{[-205, -200]}(k) & \varphi_2(k) &= \chi_{[-140, -135]}(k) \\ \varphi_3(k) &= \chi_{[-25, -20]}(k) & \varphi_4(k) &= \chi_{[-5, 0]}(k) \\ \varphi_5(k) &= \chi_{[0, 5]}(k) & \varphi_6(k) &= \chi_{[20, 25]}(k) \\ \varphi_7(k) &= \chi_{[135, 140]}(k) & \varphi_8(k) &= \chi_{[200, 205]}(k) \end{aligned}$$

to collect the frequency information in the corresponding frequency intervals and shift the center of the interval to the origin by a phase factor. For each $f_j(x) = \mathcal{F}^{-1}[\widehat{f}\varphi_j](x)$, we construct two DNNs to learn its real part and imaginary part, separately. Every DNN have 4 hidden layers and each layer has 40 neurons. Namely, the DNN has the structure 1-40-40-40-40-1. The training data is obtained by 10,000 samples from the uniform distribution on $[-\pi, \pi]$ and the testing data is 500 uniformly distributed samples. We train these DNNs by Adam optimizer with training rate 0.0002 with 10 epochs of training for each DNN. The result is shown in Fig. 1.

The detail of this training is shown in Fig. 2.

These figures clearly shows that phase DNN can capture the various high frequencies, from low frequency $\pm 1, \pm 3$ to high frequency ± 203 quite well. The training error and time of phase DNN are collected in table 1

It is shown that taking the advantage of vectorization, the convolution step costs about 20% time of training. Because in different interval, $f_j(x)$ can be trained in parallel, PhaseDNN is ideal to take advantage of parallel computing architectures.

In comparison with one single DNN, we have used a 24 hidden layers with 80 neurons per hidden layer with the same amount of training data, the loss is still around 100 after more than 5000 epoch of training taking over 22 hours nonstop running on the same workstation.

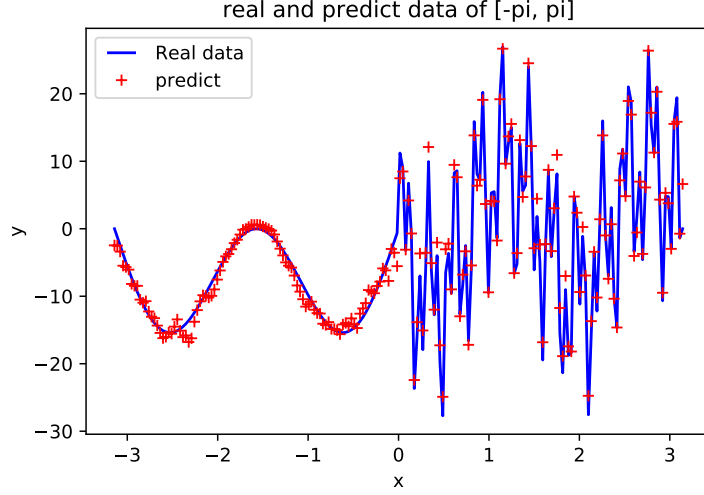


Figure 1: The testing result of $f_{DNN}(x)$ trained by phase DNN. The blue solid line is $f(x)$ and the data marked by + in red is the value of $f_{DNN}(x)$ at testing data set.

	Convolution time(s)	Training Time(s)	Training Error	Test Error
$[-205, -200]$	34.43	169.82	-	-
$[-140, -135]$	33.74	185.40	-	-
$[-25, -20]$	33.22	199.48	-	-
$[-5, 0]$	9.70	214.39	-	-
$[0, 5]$	9.78	230.46	-	-
$[20, 25]$	33.21	247.34	-	-
$[135, 140]$	33.38	263.89	-	-
$[200, 205]$	32.68	279.39	-	-
Total	220.14	1790.17	0.01508	0.06831

Table 1: The training time and error statistics. For each j , the training time is the sum of training time of real and imaginary part. For each DNN, epoch is chosen to be 10.

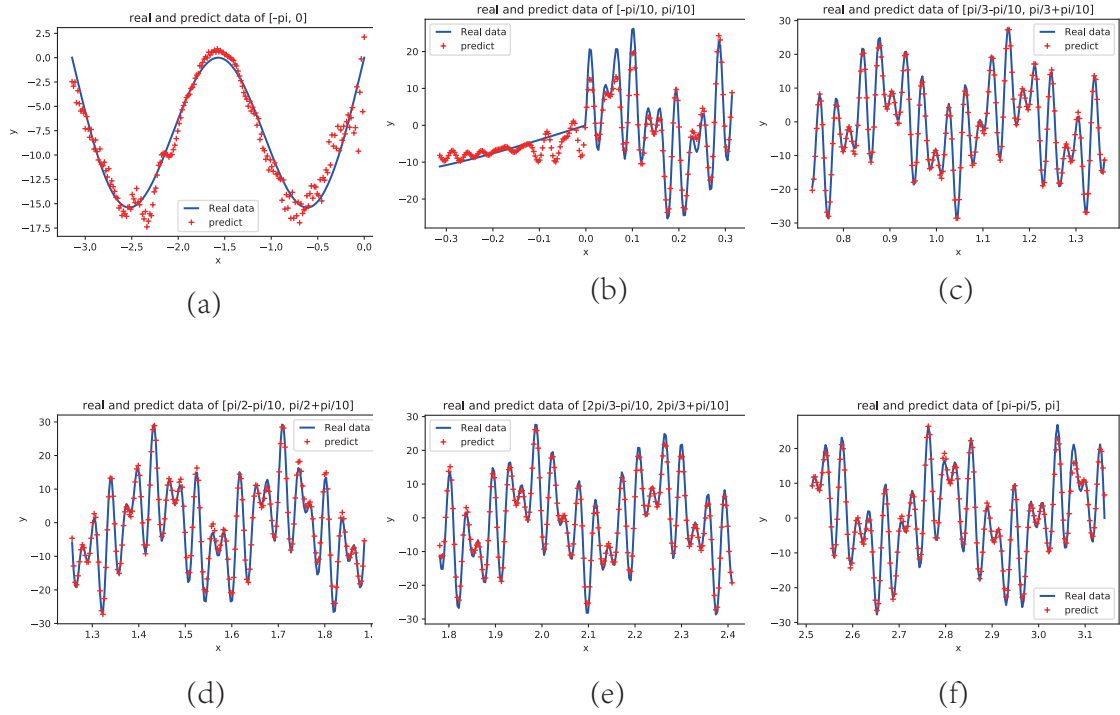


Figure 2: The detail result of training in different intervals. The subfigure (a)-(f) shows the results in interval $[-\pi, 0]$, $[-\pi/10, \pi/10]$, $[\pi/3 - \pi/10, \pi/3 + \pi/10]$, $[\pi/2 - \pi/10, \pi/2 + \pi/10]$, $[2\pi/3 - \pi/10, 2\pi/3 + \pi/10]$ and $[\pi - \pi/10, \pi]$ correspondingly. The blue solid line is $f(x)$ and the data marked by + in red is the value of $f_{DNN}(x)$ at testing data set.

5.2. Numerical results of coupled PhaseDNN

5.2.1. 1-D Problem

We will use test the coupled PhaseDNN on our previous test problems. Namely, we are going to learn

$$f(x) = \begin{cases} \sin x + \sin 3x, & \text{if } x \in [-\pi, 0] \\ \sin 23x + \sin 137x + \sin 203x, & \text{if } x \in [0, \pi]. \end{cases} \quad (34)$$

by Eqn. (28). The frequencies w_m are selected to be 0, 5, 25, 135, 200 as before. For each A_m and B_m , we set it as a 1-40-40-40-40-1 DNN.

The training parameters are as follow: we use 10000 random samples and train 40 epochs with batchsize 50. The optimizer is Adam with learning rate 0.002. The testing data is 10000 evenly distributed samples. The fitting result is shown in the left panel in Fig.3.

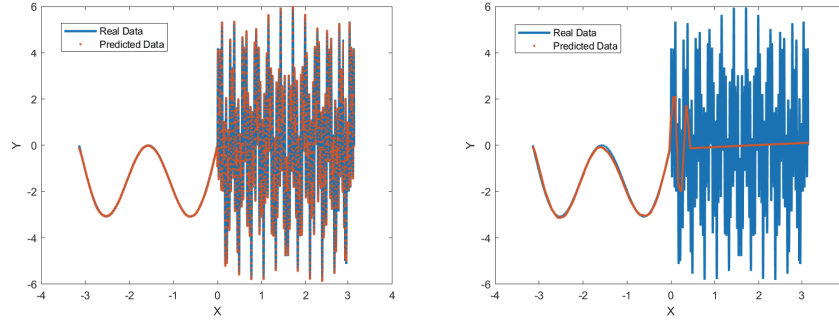


Figure 3: Fitting result for $f(x)$. We select frequency $w_n \in \{0, 5, 25, 135, 200\}$. Left panel: training result using Eqn.(28). Right panel: training result using a fully connected DNN with depth 4 and width 360.

The total training time is less than 10 seconds. The average L^2 training error and testing error are both 8.2×10^{-4} . The maximum error is 0.26. The error is concentrated in the neighborhood of 0, where the derivative of $f(x)$ is discontinuous. Out of this neighborhood, the maximum error is 0.08.

We can also sweep the frequency space by choosing the frequencies w_m to be -250:10:250, training parameters are the same as before. The fitting result and error is shown in Fig.4. The average L^2 training and testing error are reduced to 4.2×10^{-4} .

For comparison, we can also use a fully connected DNN with similar scale as Eqn.(28) to learn $f(x)$. This DNN has 4 hidden layers with 360 neuron in

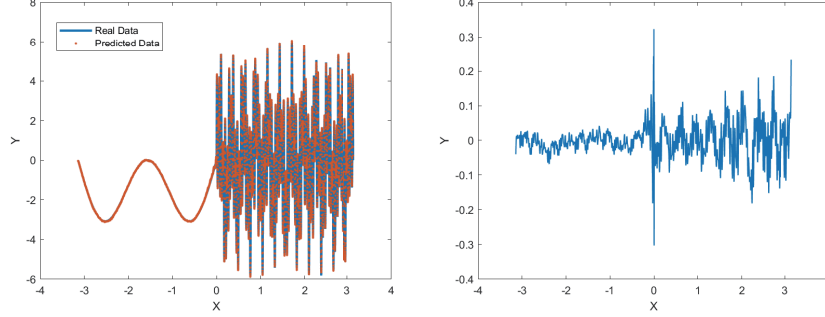


Figure 4: Fitting result for $f(x)$ using sweep method. Frequency domain is $[-250, 250]$. Left panel: fitting. Right panel: error. Fitting result for $f(x)$ using sweep method. Frequency domain is $[-250, 250]$. Left panel: fitting. Right panel: error.

each layer. This DNN was trained with the same parameter as before. The result is shown in the right panel of Fig.3. It is clear that almost nothing was learned by this fully connected DNN for this high frequency data.

In fact, 10000 samples are too many for this example, it turns out that 1000 samples can lead to a good approximation with Eqn. (28). Even with 500 samples, which is a much too small data set for the frequency 203, We can still get a ‘not too bad’ result. The testing is also done with 10000 samples. These results are shown in Fig.5.

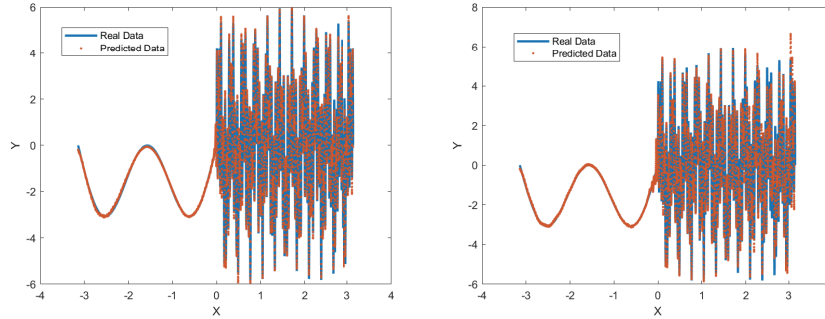


Figure 5: Fitting result for $f(x)$ using less data. We select frequency $w_n \in \{0, 5, 25, 135, 200\}$. Left panel: training with 1000 random samples. Right panel: training with 500 random samples.

Discontinuous functions and frequency sweep

Next we consider discontinuous functions and we replace the sin in Eqn.(34) by square wave function with same frequency and learn it by (28) with $w_m = 0, 5, 25, 135, 200$ and $w_m = -800 : 10 : 800$. These two DNNs are trained with 10000 samples and 100 epochs. The results are shown in Fig.6.

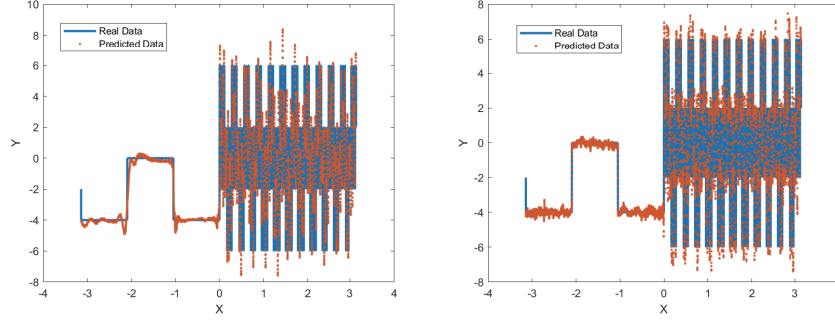


Figure 6: Fitting result for square wave function using selecting and sweeping methods. Left panel: fitting result using selecting method. Right panel: fitting result using sweeping method. Frequency domain is $[-800, 800]$.

It can be seen that although the sweeping strategy performs better than selecting, it is less accurate than the $\sin x$ case. The average L^2 error is 7×10^{-3} , maximum error is 6.

5.2.2. 2D-Problem

We use Eqn. (28) to learn 2D and 3D problems. For 2D test, the the function $G(x, y) = g(x)g(y)$ is used, where $g(x)$ is defined by

$$g(x) = \begin{cases} \sin x + \sin 3x, & \text{if } x \in [-\pi, 0] \\ \sin 23x + \sin 137x, & \text{if } x \in [0, \pi]. \end{cases} \quad (35)$$

The function $g(x)$ is the $f(x)$ in (34) without the $\sin 203x$ component. In this test, we choose $w_m \in \{0, 5, 25, 135\} \times \{0, 5, 25, 135\}$. Training setting are $640 \times 640 = 409600$ samples and 80 epochs with batchsize 100. Testing data is 100×100 . The result is shown in Fig.7.

The result is quite good even for the highest frequency domain. In this example, the highest frequency is 137. With more data, we can learn a function of even higher frequency.

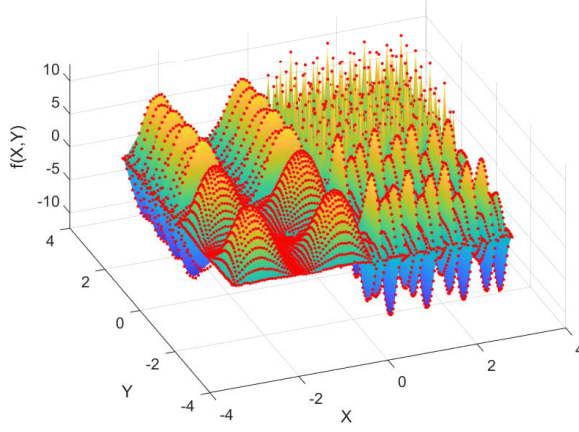


Figure 7: Fitting result for $G(x, y)$.

5.2.3. 3D-Problem

The test problem for 3D is $H(x, y, z) = h(x)h(y)h(z)$, where

$$h(x) = \begin{cases} \sin x + \sin 3x, & \text{if } x \in [-\pi, 0] \\ \sin 23x + \sin 32x, & \text{if } x \in [0, \pi]. \end{cases} \quad (36)$$

The selected frequency is $w_m = \{0, 25, 30\} \times \{0, 25, 30\} \times \{0, 25, 30\}$. Training uses $150 \times 150 \times 150 = 3375000$ random samples and 50 epoches with batchsize 1000. Because we cannot plot a 4-D picture, we choose hypersurface $z = 1$ and $x + y + z = 1$ as test data. Each A_m, B_m is chosen to be 1-20-20-20-20-1 DNN. The whole network is trained 40 epoches with batchsize 1000. This training cost about 5 hours. Results are shown in Fig.8.

Remark 5. Advantages: The main advantage of this approach is we don't need to treat convolution. This makes it possible to deal with large data set. More data can reveal higher frequency and higher dimensional. In our previous $\text{sinc}(x)$ selecting process, the convolution may introduce some numerical error. Now Eqn.(28) has no such kind of numerical error. This is another advantage.

Disadvantage: Comparing with our previous method, the main disadvantage of Eqn.(28) is it cannot be parallelized. We must choose all the w_m before training, then build DNN $T(x)$ according to these w_m . If the w_m we

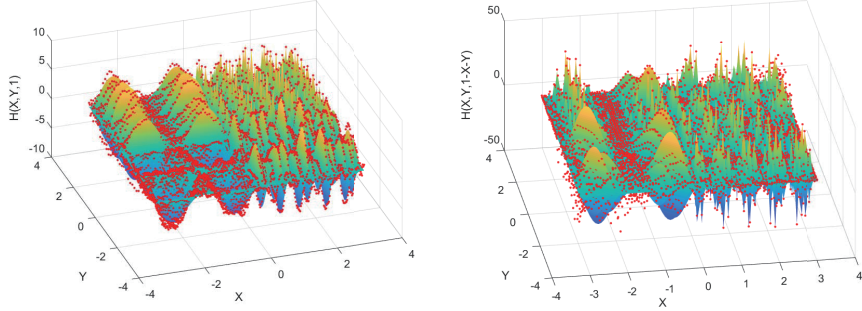


Figure 8: Fitting result for $H(x, y, z)$. Left panel: fitting result on hypersurface $z = 1$. Right panel: fitting result on hypersurface $x + y + z = 1$.

choose are not enough, we can learn the residual by some more w_m , but cannot use these w_m to train the original $f(x)$ separately.

Remark 6. The number of data. Basically, the data set must be big enough so that it can reveal all the frequencies. That means we still need $O(N^d)$ data. For each direction, N samples must reveal the highest frequency of this direction. This means, even though DNN has the advantage that the unknowns increase linearly w.r.t the number of dimension, we still need to pay exponentially computing cost, at least for computing loss function. In our 3D test, 150 random samples for each direction is merely enough for frequency 32, but the total number 3.4×10^6 is a very big data set.

The advantage that number of unknowns of DNN increase linearly also need more discussion. The traditional DNN can be viewed as a sum of a series of DNNs. F -principle tells the main part of a single DNN in Fourier space concentrates in a neighborhood of 0. If we agree with the small parameter assumption, one cannot approximate a function who has a support far away from 0. Our approach Eqn.(28) uses phase shifting technique. The main part of $T(x)$ in Fourier space lies in the neighborhood of each w_m . It seems we build a mesh in Fourier space w.r.t w_m implicitly. Like in my 3D test, the mesh is $\{-30, -25, 5, 0, 5, 25, 30\} \times \{-30, -25, 5, 0, 5, 25, 30\} \times \{-30, -25, 5, 0, 5, 25, 30\}$.

It can be seen that our approach cannot overcome curse of dimensionality either, since generally, the number of w_m also increase exponentially. In our 3D test problem, there are 108 different w_m , which corresponds to 216 small

DNNs. The whole DNN $T(x)$ has a width over 4000. It is a very wide and shallow DNN. The number of parameters is very large. Combining a large number of data, the whole training costs 5 hours.

However, we only need to apply the coupled PhaseDNN for the 3 physical dimension of the solution while the other dimensions from the random coefficients can be handled by normal DNN.

5.3. Coupled PhaseDNN for solving Helmholtz equations in inhomogeneous media

5.3.1. Helmholtz equation with constant wave numbers

We set $w_m \in \{0, \lambda, \mu\}$, each A_m, B_m to be 1-40-40-40-1 DNN. The whole $T(x)$ is trained with 10000 evenly distributed samples, 100 epochs and batchsize 100. We choose four special cases: $\lambda = 3, \mu = 2$, $\lambda = 200, \mu = 2$, $\lambda = 2, \mu = 200$ and $\lambda = 300, \mu = 200$. The result is shown in Fig.9.

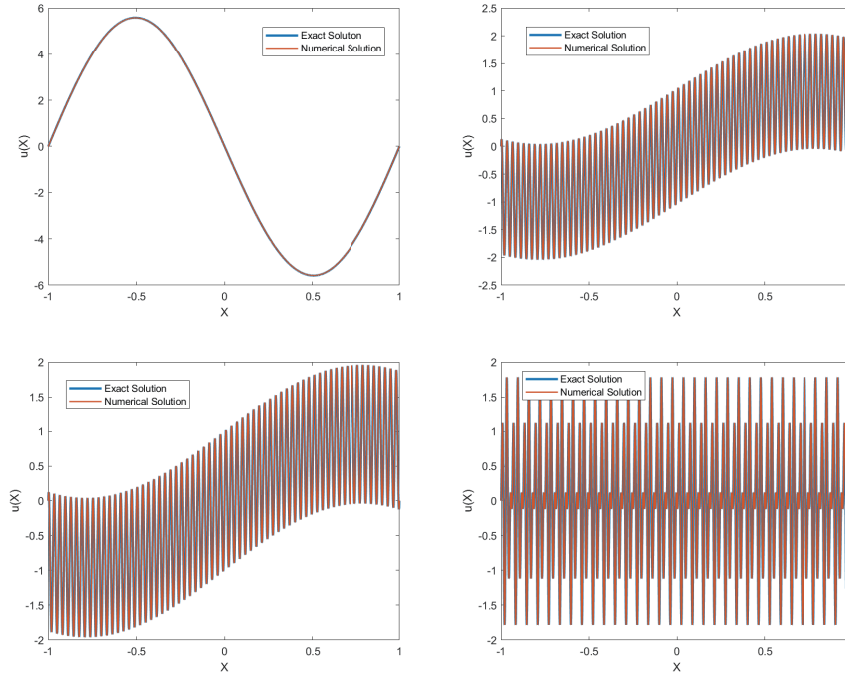


Figure 9: Numerical and exact solution of Eqn.(29) with different λ and μ . Upper left panel: $\lambda = 3, \mu = 2$. Upper right panel: $\lambda = 200, \mu = 2$. Lower left panel: $\lambda = 2, \mu = 200$. Lower right panel: $\lambda = 300, \mu = 200$.

The training costs about 5 minute. The maximum error is $O(10^{-4})$. The results are quite accurate. For comparison, a single fully connected DNN with similar scale as $T(x)$ cannot solve the equation at all. The training result after 1500 epochs for $\lambda = 3, \mu = 2$ and $\lambda = 200, \mu = 2$ are shown in Fig.10, showing the non-convergence of the usual fully connected DNN.

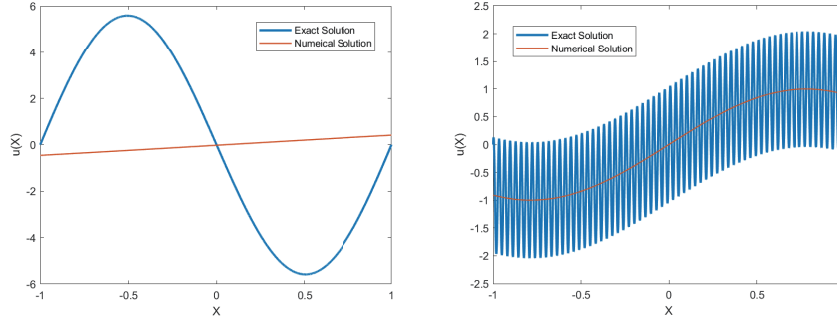


Figure 10: Non-convergence of usual fully connected DNN: DNN and exact solution of Eqn.(29) with different λ and μ . Left panel: $\lambda = 3, \mu = 2$. Right panel: $\lambda = 200, \mu = 2$.

5.3.2. Helmholtz Equation with variable wave numbers

Next we are going to solve the following Helmholtz equations with variable wave numbers

$$\begin{cases} u'' + (\lambda^2 + c \sin(mx^2))u = (\lambda^2 - \mu^2) \sin(\mu x) \\ u(-1) = u(1) = 0, \end{cases} \quad (37)$$

where $c > 0, m > 0$ are constants.

As there is no explicit exact solution to this equation, the numerical solution obtained by finite difference method will be used as the reference solution.

We first choose $\lambda = 100, \mu = 10, c = 10$ and $m = 1$ in Eqn.(37), which corresponds to a low frequency external wave source and a low wave number with small background media inhomogeneity. In the coupled phaseDNN, we choose $w_m \in \{0, 10 : 10 : 150\}$. Other training parameters are set to be similar as in the constant coefficient case. The numerical result of coupled phaseDNN and reference solution is shown in Fig11 and the absolute error is in the order of $O(10^{-3})$.

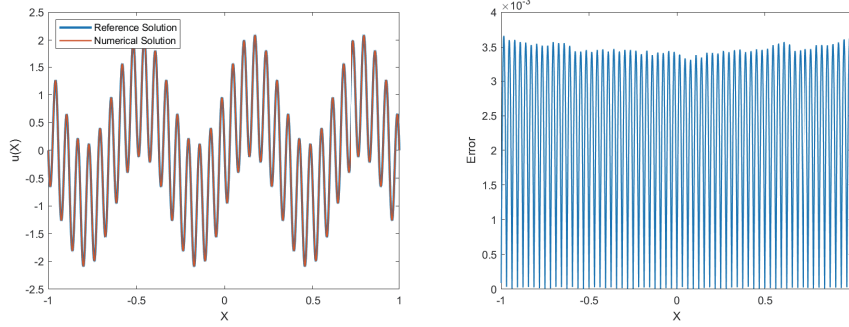


Figure 11: Numerical and exact solution of Eqn.(37) using coupled phaseDNN $\lambda = 2$, $\mu = 10$, $c = 3.6$ and $m = 1$. Left panel: The numerical solution and reference solution obtained by finite difference method. Right panel: The absolute value of the difference between numerical solution and reference solution.

Next, We choose $\lambda = 2$, $\mu = 200$, $c = 0.9\lambda^2 = 3.6$ and $m = 1$ in Eqn.(37), which corresponds to a high frequency external wave source and a low wave number with small background media inhomogeneity. In coupled phaseDNN, we choose $w_m \in \{1, 2, 3, 4, 200\}$. Other training parameters are set to be similar as in the constant coefficient case. The numerical result of coupled phaseDNN and reference solution is shown in Fig12 and the absolute error is in the order of $O(10^{-3})$.

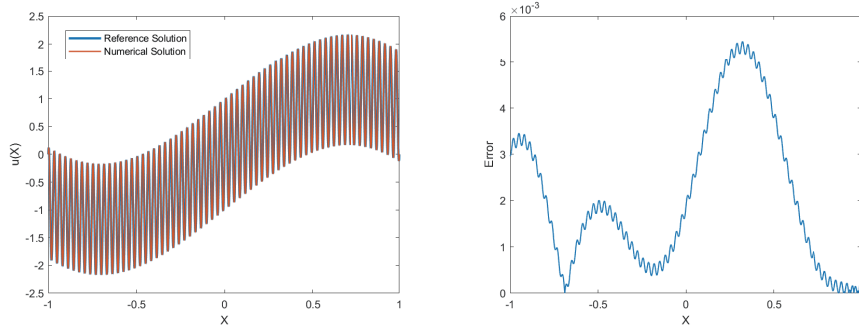


Figure 12: Numerical and exact solution of Eqn.(37) using coupled phaseDNN $\lambda = 2$, $\mu = 200$, $c = 3.6$ and $m = 1$. Left panel: The numerical solution and reference solution obtained by finite difference method. Right panel: The absolute value of the difference between numerical solution and reference solution.

We further choose $\lambda = 100$, $\mu = 200$, $c = 10$ and $m = 1$, which corre-

sponds to a high frequency external wave source and a high wave number with larger background media inhomogeneity. w_m is chosen to be 0 and 100 : 10 : 300. The result is shown in Fig.13 and the absolute error is in the order of $O(10^{-3})$.

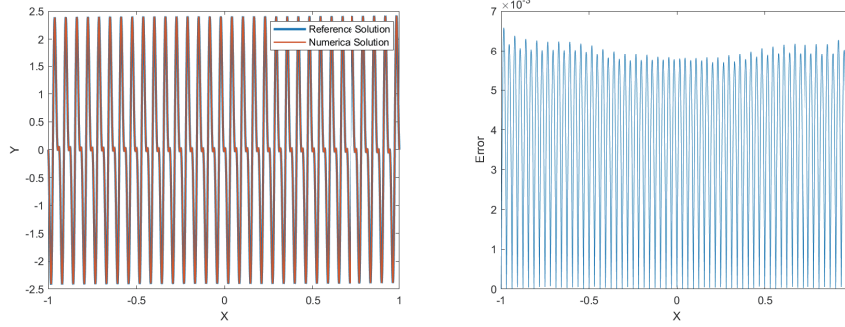


Figure 13: Numerical and exact solution of Eqn.(37) using coupled phaseDNN $\lambda = 100$, $\mu = 200$, $c = 10$ and $m = 1$. Left panel: The numerical solution and reference solution obtained by finite difference method. Right panel: The absolute value of the difference between numerical solution and reference solution.

It can be seen that coupled phaseDNN can handle both small and large wave numbers λ and low and high frequency external sources. The absolute error are all in the order of $O(10^{-3})$ for the test cases.

6. Conclusion

In this paper, we have proposed a phase shift DNN to learn high frequency information by using frequency shifts to convert the high frequency learning to low frequency learning. As shown by various numerical tests, this approach increases dramatically the capability of the DNN as a viable tool for solving high frequency wave differential equations in inhomogeneous media.

For future work, we will further develop the PhaseDNN to handle the high dimensionality issues from possibly random inhomogeneous media.

Acknowledgement

This work was supported by US Army Research Office (Grant No. W911NF-17-1-0368).

References

- [1] Wei Cai, Xiaoguang Li, Lizuo Liu, PhaseDNN – A Parallel Phase Shift Deep Neural Network for Adaptive Wideband Learning, arxiv 1905.01389, May 3, 2019.
- [2] Weinan, E., and Bing Yu. "The Deep Ritz method: A deep learning-based numerical algorithm for solving variational problems." *Communications in Mathematics and Statistics* 6.1 (2018): 1-12.
- [3] Xu, Zhi-Qin John, Understanding training and generalization in deep learning by Fourier analysis, arXiv:1808.04295, November, 2018.
- [4] Xu, Zhi-Qin John, Yaoyu Zhang, Tao Luo, Yanyang Xiao, and Zheng Ma. Frequency Principle: Fourier Analysis Sheds Light on Deep Neural Networks. arXiv preprint arXiv:1901.06523 (2019).
- [5] Brandt, Achi. Multi-level adaptive solutions to boundary-value problems. *Mathematics of computation* 31.138 (1977): 333-390.
- [6] Wei Cai, Xiaoguang Li, Lizuo Liu, PhaseDNN - A Parallel Phase Shift Deep Neural Network for Adaptive Wideband Learning, arxiv 1905.01389, May 3, 2019.
- [7] Daubechies, Ingrid. Ten lectures on wavelets. Vol. 61. Siam, 1992.
- [8] Cai, Wei, and Jianzhong Wang. Adaptive multiresolution collocation methods for initial-boundary value problems of nonlinear PDEs. *SIAM Journal on Numerical Analysis* 33, no. 3 (1996): 937-970.
- [9] Wendland, Holger. Scattered data approximation. Vol. 17. Cambridge university press, 2004.